A 3-Dimensional Bergman Kernel Method with Applications to Rectangular Domains

S. Bock[†], M. I. Falcão[‡1], K. Gürlebeck[†] and H. Malonek[*]

[†] *Bauhaus-Universität Weimar, Institut Mathematik/Physik, D-99421 Weimar, Germany*

[‡] *Centro de Matemática, Universidade do Minho, 4710-057 Braga, Portugal*

[*] *Departamento de Matemática, Universidade de Aveiro, 3810-193 Aveiro, Portugal*

Abstract

In this paper we revisit the so-called Bergman kernel method - BKM - for solving conformal mapping problems and propose a generalized BKM-approach to extend the theory to 3-dimensional mapping problems. A special software package for quaternions was developed for the numerical experiments.

AMS classification: 30C30, 65E05.

Keywords Numerical Conformal Mapping, Bergman Kernel, Quaternions.

[1]Email: mif@math.uminho.pt

Research partially supported by the Portuguese Foundation for Science and Technology - FCT through the research program POCTI

1 Introduction

The construction of reproducing kernel functions is not restricted to real 2-dimension. Indeed, the two complex variable case has been already considered by Bergman himself (cf.[1]). Moreover, results concerning (and restricted to) the construction of Bergman kernel functions in closed form for special domains in the framework of hypercomplex function theory can be found in [4, 5, 13, 14].

They suggest that the well known Bergman kernel method - BKM - can also be extended to mapping problems in higher dimensions, particularly 3-dimensional cases. We illustrate such a generalized BKM-approach by presenting numerical examples obtained by the use of specially developed software packages for quaternions.

2 The complex case revisited

Let Ω be a bounded simply-connected domain with boundary $\partial\Omega$ in the complex z–plane ($z = x + iy$), and let $L^2(\Omega)$ denote the Hilbert space of all square integrable functions which are analytic in Ω. Consider the inner product in $L^2(\Omega)$

$$< g_1(z), g_2(z) >= \iint_\Omega g_1(z)\overline{g_2(z)}dxdy,$$

assume w.l.o.g. that $0 \in \Omega$ and let $K(.,0)$ be the Bergman kernel function of Ω with respect to 0. Then, the kernel function $K(.,0)$ is uniquely characterized by the *reproducing property*, i.e.

$$< g, K(.,0) >= g(0),\ \forall g \in L^2(\Omega).$$

There are several methods for solving conformal mapping problems. In contrast to most conformal mapping techniques, the approximation of the solution obtained by using the Bergman kernel method is an analytic function.

The BKM is a method for approximating the mapping f which maps conformally Ω onto the unit disc $D := \{w : |w| < 1\}$, in such a way that $f(0) = 0$ and $f'(0) > 0$. The method is based on the *reproducing property* (2) of the kernel function and on the well known relation of $K(.,0)$ with f,

$$f(z) = \sqrt{\frac{\pi}{K(0,0)}} \int_0^z K(t,0)dt, \tag{2.1}$$

(see [1, 6, 7]). More precisely, the BKM involves the following four steps:

S1 Choose a complete set of functions $\{\eta_j\}_1^\infty$ for the space $L^2(\Omega)$.

S2 Orthonormalize the functions $\{\eta_j\}_1^n$ by means of the Gram-Schmidt process to obtain an orthonormal set $\{\eta_j^*\}_1^n$.

S3 Approximate the kernel function $K(.,0)$ by the Fourier sum

$$K_n(z,0) = \sum_{j=1}^{n} < K(.,0), \eta_j^* > \eta_j^*(z) = \sum_{j=1}^{n} \overline{\eta_j^*(0)}\eta_j^*(z) \tag{2.2}$$

S4 Approximate f by

$$f_n(z) = \sqrt{\frac{\pi}{K_n(0,0)}} \int_0^z K_n(t,0)dt. \tag{2.3}$$

The second step of the BKM involves the use of the Gram-Schmidt process which can be extremely unstable and demands high accuracy. Methods to circumvent such instability problems are described in [10, 12]. Another way to avoid this numerical problem is to use, whenever it is possible, for example Maple, as this system provides integration routines so that the inner products involved in the construction of the Gramian matrix can be computed without any loss of accuracy (cf. [9]).

3 From $\mathbb{C}$ to $\mathbb{H}$

Let $\{1, e_1, e_2, e_3\}$ be an orthonormal base of the Euclidean vector space $\mathbb{R}^4$ with a product according to the multiplication rules

$$e_1^2 = e_2^2 = e_3^2 = -1, \;\; e_1e_2 = -e_2e_1 = e_3.$$

This non-commutative product generates the algebra of real quaternions $\mathbb{H}$. The real vector space $\mathbb{R}^4$ will be embedded in $\mathbb{H}$ by identifying the element

$$x = (x_0, x_1, x_2, x_3) \in \mathbb{R}^4$$

with the element

$$q = x_0 + e_1x_1 + e_2x_2 + e_3x_3 \in \mathbb{H}.$$

The conjugate of q is

$$\bar{q} = x_0 - e_1x_1 - e_2x_2 - e_3x_3.$$

Instead of the real and the imaginary parts we will distinguish between the scalar part of q

$$\text{Sc } q := x_0 = \frac{1}{2}(q + \bar{q})$$

and the vector part of q

$$\text{Vec } q := e_1 x_1 + e_2 x_2 + e_3 x_3 = \frac{1}{2}(q - \bar{q}).$$

The norm $|q|$ of q is defined by

$$|q|^2 = q\bar{q} = \bar{q}q = x_0^2 + x_1^2 + x_2^2 + x_3^2$$

and it immediately follows that each non-zero $q \in \mathbb{H}$ has an inverse given by

$$q^{-1} = \frac{\bar{q}}{|q|^2}.$$

Introducing the hypercomplex variables

$$z_1 = -\frac{qe_1 + e_1 q}{2} = x_1 - e_1 x_0$$

and

$$z_2 = -\frac{qe_2 + e_2 q}{2} = x_2 - e_2 x_0,$$

we get

$$\mathbb{H}^2 = \{(z_1, z_2) : z_1 = x_1 - e_1 x_0,\ z_2 = x_2 - e_2 x_0\} \cong \mathbb{R}^3 \cong \mathcal{A} := \text{span}_{\mathbb{R}}\{1, e_1, e_2\}.$$

Now, let Ω be a domain in $\mathbb{R}^3$ and consider the $\mathbb{H}$-valued function defined in Ω:

$$f : \mathbb{R}^3 \to \mathbb{R}^4 \cong \mathbb{H}$$

$$f(x) = f_0(x) + e_1 f_1(x) + e_2 f_2(x) + e_3 f_3(x),$$

where $x = (x_0, x_1, x_2) \in \mathbb{R}^3$ and f_k are real valued in Ω functions. On the set $C^1(\Omega, \mathbb{H})$ define the quaternionic Cauchy-Riemann operator

$$D = \frac{\partial}{\partial x_0} + e_1 \frac{\partial}{\partial x_1} + e_2 \frac{\partial}{\partial x_2}$$

and its conjugate

$$\bar{D} = \frac{\partial}{\partial x_0} - e_1 \frac{\partial}{\partial x_1} - e_2 \frac{\partial}{\partial x_2}.$$

Definition 1 *A C^1-function f is called left-monogenic (resp. right-monogenic) in a domain Ω if*

$$Df = 0, \text{ in } \Omega \qquad (\text{ resp. } fD = 0 \text{ in } \Omega).$$

Definition 2 *If $\vec{z} = (z_1, z_2)$ then the "symmetric power ν" of $\vec{z}$ is defined as*

$$\vec{z}^{\nu} := {z_1}^{\nu_1} \times {z_2}^{\nu_2} = \frac{\nu!}{|\nu|!} \sum_{\prod(i_1,\cdots,i_{|\nu|})} z_{i_1} \cdots z_{i_{|\nu|}},$$

where $\nu = (\nu_1, \nu_2)$ is a multi-index, $|\nu| = \nu_1 + \nu_2$, $\nu! = \nu_1!\nu_2!$ and the sum is taken over all permutations of $(i_1, \cdots, i_{|\nu|})$.

Proposition 1 *([11]) The permutational product ${z_1}^{\nu_1} \times {z_2}^{\nu_2}$ satisfies the recursion formula*

$$z_1^{\nu_1} \times {z_2}^{\nu_2} = \frac{1}{\nu_1 + \nu_2}\{\nu_1(z_1^{\nu_1 - 1} \times z_2^{\nu_2})z_1 + \nu_2(z_1^{\nu_1} \times z_2^{\nu_2 - 1})z_2\}.$$

Proposition 2 *([3, 11]) Let $H_\nu^k(\vec{z}) := {z_1}^{\nu_1} \times {z_2}^{\nu_2}$, with $|\nu| = k$.*

1. *$H_\nu^k(\vec{z})$ are homogeneous polynomials of degree k.*
2. *$H_\nu^k(\vec{z})$ are monogenic functions.*
3. *$\{H_\nu^k(\vec{z})\} \cup \{1\}$ is a linearly independent system, for each $k \in \mathbb{N}$.*

(These polynomials are also called Fueter-polynomials).

4 A 3-Dimensional Bergman Kernel Method

The construction of reproducing kernel functions is not restricted to real dimension 2. Nowadays, reproducing kernels are a well known tool in the theory of functions of one or several complex variables and also in Clifford Analysis (for a review see [3, 8]). For more practical applications it is necessary to know the reproducing kernel explicitly. Results concerning the construction of Bergman kernel functions in closed form for special domains (the ball, the half-plane, strip domains, rectangular domains, etc) can be found in [3, 4, 5, 13, 14]. In this paper we construct the Bergman kernel function numerically and propose an analogous BKM for 3 dimensional cases.

Let Ω be a bounded simply-connected domain in $\mathbb{R}^3$ and denote by $L^2_r(\Omega, \mathbb{H})$ the right-Hilbert space of all square integrable $\mathbb{H}$-valued functions, depending on $x = (x_0, x_1, x_2) \in \Omega$, endowed with the inner product,

$$< f(x), g(x) >= \int_\Omega \overline{f(x)} g(x)\, dV. \tag{4.4}$$

The right linear set $L^2_r(\Omega, \mathbb{H}) \cap \ker D$ is a subspace in $L^2_r(\Omega, \mathbb{H})$ and has also a unique reproducing kernel $K(x, \zeta)$, i.e

$$< K(., \zeta), f >= f(\zeta),\ \forall f \in L^2_r(\Omega, \mathbb{H}) \cap \ker D.$$

If we now take an orthonormal complete system of functions $\{\eta^*_j\}$ then it can be proved that a Fourier series expansion exists for all functions $f \in L^2_r(\Omega, \mathbb{H}) \cap \ker D$

$$f(x) = \sum_{j=1}^{\infty} \eta^*_j(x) < \eta^*_j, f >$$

and therefore

$$K(x, \zeta) = \sum_{j=1}^{\infty} \eta^*_j(x) < \eta^*_j, K(x, \zeta) >= \sum_{j=1}^{\infty} \eta^*_j(x) \overline{\eta^*_j(\zeta)},$$

(see, for example [3, 8] for details).

This result suggests a numerical procedure to construct approximations to K similar to the complex case. More precisely, and assuming w.l.o.g. that $0 \in \Omega$, we rewrite steps **S1-S3** of BKM as follows:

S1 Choose a complete set of functions $\{\eta_j\}_1^\infty$ for the space $L^2_r(\Omega, \mathbb{H}) \cap \ker D$.

In the complex case, the usual choice of the basis set is to consider the non-negative powers of z. Unfortunately, if $z = x_0 + e_1 x_1 + e_2 x_2 + e_3 x_3 \in \mathbb{H}$, these polynomials are not monogenic. However, it is well known that the monogenic Fueter polynomials introduced in Section 3.1, H^k_ν, $|\nu| = k$; $k = 0, 1, \cdots$, are a complete set of functions and are therefore the natural choice in this step.

S2 Orthonormalize the functions $\{\eta_j\}_1^n$ by means of the Gram-Schmidt process to obtain an orthonormal set $\{\eta^*_j\}_1^n$.

The use of Fueter polynomials up to degree N corresponds to a total of

$$n := \frac{(N+1)(N+2)}{2}$$

functions. More precisely, the n homogeneous polynomials of degree $k \leq N$ are

$$\eta_j := H^k_{k-i,i};\ k = 0, \cdots N;\ i = 0, \cdots, k;\ j = \frac{k(k+1)}{2} + i + 1.$$

S3 Approximate the kernel function $K(., 0)$ by the Fourier sum

$$K_N(x, 0) = \sum_{j=1}^{n} \eta_j^*(x)\overline{\eta_j^*(0)};\ N = 0, 1, \cdots$$

All these results underline that Clifford analysis and one complex variable analysis are closely connected. Thus, if we go further and introduce

S4 Compute

$$f_N(x) = C_N \int_0^x K_N(t, 0)dt;\ N = 0, 1, \cdots,$$

where C_N denotes some appropriate constant (depending on $K_N(0, 0)$), shall we get an approximation to a mapping function f from the original domain Ω onto the unit ball $\mathcal{B}$ in $\mathbb{R}^3$?

Before attempting to answer this question, we should make some remarks.

Remark 1 *We can not expect f to be conformal, in the sense of Gauss, as it is well known that in $\mathbb{R}^3$ the set of conformal mappings is restricted to the set of Möbius transformations as firstly shown by J. Liouville in 1850. Nevertheless, the use of a monogenic set of functions η_j for constructing K_N suggests that the mapping function itself should have some special properties.*

Remark 2 *The polynomials η_j are in $\Omega \subset \mathbb{R}^3 \cong \mathcal{A} :=$ span $_{\mathbb{R}}\{1, e_1, e_2\}$, but the corresponding orthonormal polynomials η_j^* are, in general, in $\mathbb{H} \cong \mathbb{R}^4$. This means that the kernel function K and the mapping function f are, in general, functions from Ω in $\mathbb{R}^4$.*

Remark 3 *From the geometric and practical point of view, we would like f to map domains $\Omega \subset \mathbb{R}^3$ to a ball in $\mathbb{R}^3$.*

The next two results are the starting point for the numerical BKM we propose. The corresponding proofs can be obtained easily, after some manipulation, by using the definition of monogenic functions.

Lemma 1 *If a function f of the form*

$$f = f(x) = f_0(x) + f_1(x)e_1 + f_2(x)e_2,$$

is left-monogenic then f is also right-monogenic.

Lemma 2 *Let $f : \Omega \subset \mathbb{H}^2 \to \mathbb{H} \cong \mathbb{R}^4$ be a function of the form*

$$f = f(x) = f_0(x) + f_1(x)e_1 + f_2(x)e_2 + f_3(x)e_3,$$

monogenic from both sides and such that $0 \in f(\Omega)$. Then,

$$f_3 = 0, \;\; \textit{i.e.} \;\; f : \mathbb{H}^2 \to \mathcal{A} \cong \mathbb{R}^3.$$

We underline that we don't expect f to be monogenic from both sides. We recall that quaternionic Möbius transformations themselves are neither left nor right monogenic. Moreover, the kernel function itseft is left monogenic, but, in general, it is not right monogenic. However, Lemma 1 and Lemma 2 give the motivation for the numerical procedure we propose for computing f in step **S4** of BKM.

S4.1 Approximate the mapping function $g : \Omega \to \mathbb{H}$ by

$$g_N(x) = \int_0^x K_N(t, 0)dt; \; N = 1, 2, \cdots \tag{4.5}$$

S4.2 Approximate the mapping function f by "cutting" the "e_3-part" in (4.5), i.e. if g_N is of the form

$$g_N(x) = g_N^{\{0\}}(x) + g_N^{\{1\}}(x)e_1 + g_N^{\{2\}}(x)e_2 + g_N^{\{3\}}(x)e_3, \tag{4.6}$$

then construct the function f_N from Ω into $\mathcal{A} \cong \mathbb{R}^3$ by means of

$$f_N(x) = g_N^{\{0\}}(x) + g_N^{\{1\}}(x)e_1 + g_N^{\{2\}}(x)e_2. \tag{4.7}$$

The integral (4.5) is not path independent. In all what follows we integrated along the straight line from 0 to x.

In this work, we use rectangular domains to illustrate the BKM we propose, as in this case the kernel function is known exactly (see [4]) and therefore it is possible to evaluate the accuracy of the numerical procedure up to step **S3**.

Although we don't have final theoretical results, all the numerical experiments performed lead to several observations. More precisely, if Ω is a rectangular domain and if f_N and g_N are the corresponding approximations (4.5) and (4.7) to f and g, obtained in step **S4** of BKM, then we claim that,

(i) $\lim_{N\to\infty} g_N^{\{3\}}(x) = 0$.

(ii) If $C_N = \left(\dfrac{4\pi}{3K(0,0)^2}\right)^{\frac{1}{3}}$ then $\lim_{N\to\infty} ||f_N(x)|| = 1,\ x \in \partial\Omega$.

(iii) f is a conformal mapping on each side of $\partial\Omega$.

5 Numerical Examples

In this section we present numerical evidences that support the above conjectures. All the numerical results presented in this work were obtained by using a specially developed Maple software package [2].

Example 1. Consider the cube

$$\Omega_1 := \{(x_0, x_1, x_2) \in \mathbb{R}^3 : |x_0| < 1/2,\ |x_1| < 1/2,\ |x_2| < 1/2\},$$

and denote, as usual, by z_1 and z_2 the homogeneous polynomials $z_1 = x_1 - x_0 e_1$ and $z_2 = x_2 - x_0 e_2$. For example, for $N = 2$, the BKM details are as follows:

1. The 6 homogeneous polynomials of degree ≤ 2 are:

$$\eta_1 := H^0_{(0,0)}(z_1, z_2) = 1,$$
$$\eta_2 := H^1_{(1,0)}(z_1, z_2) = x_1 - x_0 e_1,$$
$$\eta_3 := H^1_{(0,1)}(z_1, z_2) = x_2 - x_0 e_2,$$
$$\eta_4 := H^2_{(2,0)}(z_1, z_2) = x_1^2 - x_0^2 - 2x_0 x_1 e_1,$$
$$\eta_5 := H^2_{(1,1)}(z_1, z_2) = x_1 x_2 - x_0 x_2 e_1 - x_0 x_1 e_2,$$
$$\eta_6 := H^2_{(0,2)}(z_1, z_2) = x_2^2 - x_0^2 - 2x_0 x_2 e_2.$$

2. The corresponding orthonormal polynomials are:

$$\eta_1^* = 1,$$
$$\eta_2^* = \sqrt{6}(x_1 - x_0 e_1),$$

$$\eta_3^* = \sqrt{2}(2x_2 - x_0e_2 + x_1e_3),$$

$$\eta_4^* = \tfrac{6}{7}\sqrt{35}(x_1^2 - x_0^2 - 2x_0x_1e_1),$$

$$\eta_5^* = \tfrac{3}{14}\sqrt{7}(14x_1x_2 - 14x_0x_2e_1 - 4x_0x_1e_2 + (5x_1^2 - 5x_0^2)e_3),$$

$$\eta_6^* = \tfrac{3}{2}\sqrt{5}(-x_0^2 - x_1^2 + 2x_2^2 - 2x_0x_2e_2 + 2x_1x_2e_3).$$

3. The approximation K_2 to the Bergman kernel function is $K_2(x,0) = 1,\ x \in \Omega_1$.

4. The approximation f_2 to the mapping function is $f_2(x) = \left(\dfrac{4\pi}{3}\right)^{\frac{1}{3}} x,\ x \in \Omega_1$.

The next figures correspond to the plots obtained with BKM for several values of N.

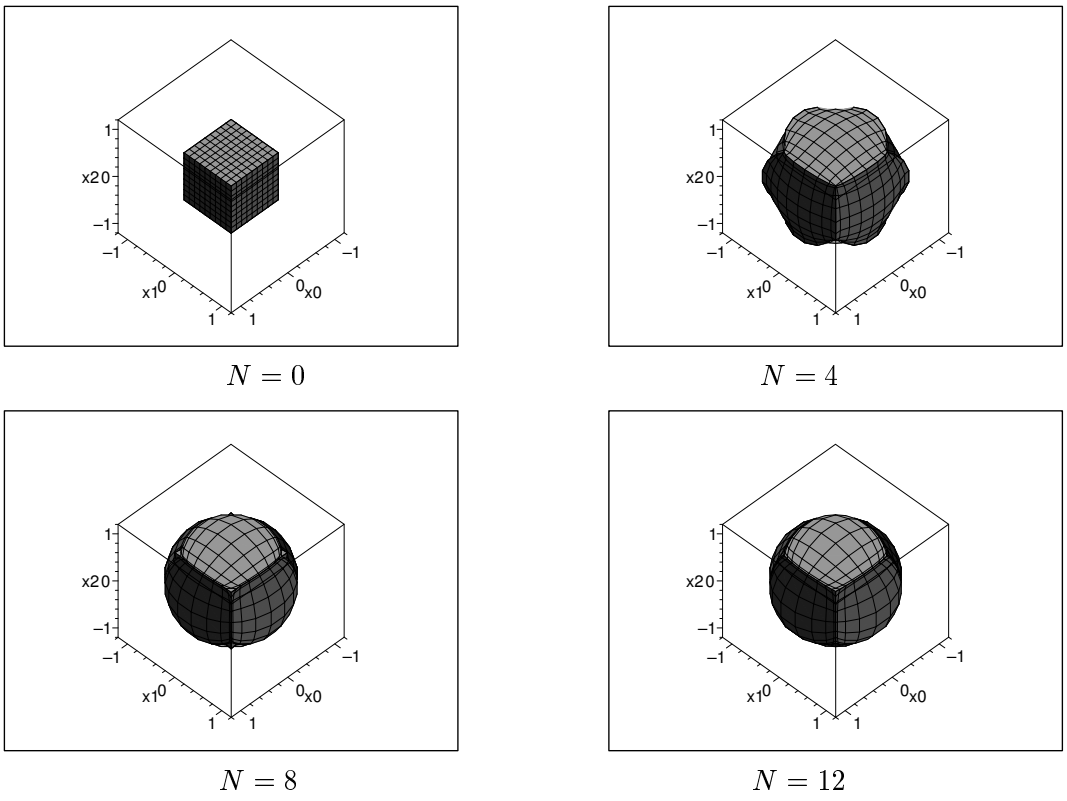

$N = 0$ $N = 4$

$N = 8$ $N = 12$

Figure 1. BKM images of the cube Ω_1

The analysis of the "e_3-part" in (4.6), i.e. $g_N^{\{3\}}(x)$ leads to the conjecture that the sequence of e_3-coordinates converges to zero. However we did not go further than $N = 12$, as our program becomes very time consuming. Figure 2 corresponds to the plot of $g_{12}^{\{3\}}(x),\ x \in \mathcal{S}$, where

$$\mathcal{S} := \{(x_0, x_1, x_2) \in \mathbb{R}^3 : |x_0| < 1/2, |x_1| < 1/2, x_2 = 1/2\}.$$

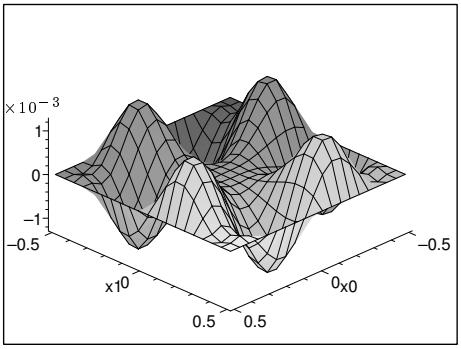

Figure 2. The function $g_{12}^{\{3\}}(x),\ x \in \mathcal{S}$.

For the same side $\mathcal{S}$ of the cube, the graphic of the error function

$$\varepsilon_N(x) := 1 - ||f_N(x)||,\ x \in \mathcal{S},$$

leads to the conclusion that the image of the cube Ω_1 seems, in fact, to be the unit ball, see Figure 3.

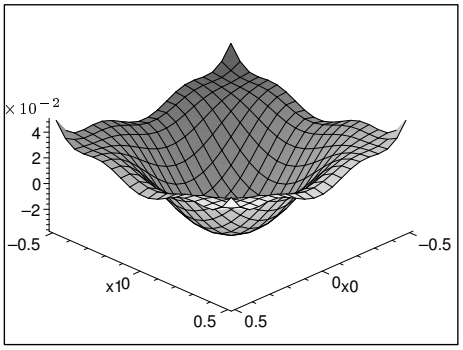

Figure 3. The function $\varepsilon_{12}(x),\ x \in \mathcal{S}$.

Moreover, by sampling the functions $g_{12}^{\{3\}}(x)$ and $\varepsilon_{12}(x)$ at a number of test points on $\mathcal{S}$, we find that

$$\max_{x \in \mathcal{S}} |g_{12}^{\{3\}}(x)| \leq 1.3 \times 10^{-3}$$

and

$$\max_{x \in \mathcal{S}} |\varepsilon_{12}(x)| \leq 4.9 \times 10^{-2}.$$

These values agree with the accuracy of the numerical approximations to the kernel function. In fact, by using the results of [4], it is possible to estimate the errors $\kappa_N(x),\ N = 0,\ 4,\ 8,\ \cdots$ in the approximations $K_N(x, 0)$ to the kernel function. For example, for $x = 0$, the values $\kappa_N(0)$ are as follows:

N	0	4	8	12
$\kappa_N(0)$	2.8×10^{-1}	6.8×10^{-2}	3.9×10^{-3}	1.5×10^{-4}

Table 1.

Finally, in our last conjecture we claim that f is a conformal mapping on each side of $\partial\Omega$. This means that, in particular, the images of orthogonal grid lines are also orthogonal on the unit sphere. The influence of the edges of the cube is visible in all plots of Figure 1 and to see this numerically, we draw an uniform 20×20 orthogonal grid on

$$\mathcal{S}(\alpha) := \{(x_0, x_1, x_2) \in \mathbb{R}^3 : |x_0| < \alpha, |x_1| < \alpha, x_2 = 1/2\},$$

for $\alpha = 0.4, 0.3, 0.2, 0.1$ and measure the associated 400 angles. The results are listed in Table 2, where we used $\mathcal{P}_\alpha$ for denoting the relative frequency of each interval. Due to the symmetry of $\mathcal{S}(\alpha)$, the corresponding subintervals in $(95, 145)$ have similar results.

$Intervals$ $(^\circ)$	$\mathcal{P}_{0.4}$	$\mathcal{P}_{0.3}$ $(\%)$	$\mathcal{P}_{0.2}$	$\mathcal{P}_{0.1}$
$(35, 45)$	2.5	$--$	$--$	$--$
$(45, 55)$	6.0	$--$	$--$	$--$
$(55, 65)$	5.5	3.0	$--$	$--$
$(65, 75)$	8.5	7.5	$--$	$--$
$(75, 85)$	12.0	17.5	13.0	$--$
$(85, 95)$	31.0	44.0	74.0	100

Table 2.

Example 2. Consider now the rectangular domain

$$\Omega_2 := \{(x_0, x_1, x_2) \in \mathbb{R}^3 : |x_0| < 1/2,\ |x_1| < 1/2,\ |x_2| < 3/4\}.$$

The next figures correspond to the plots obtained with BKM for $N = 0,\ 2,\ 6,\ 12$.

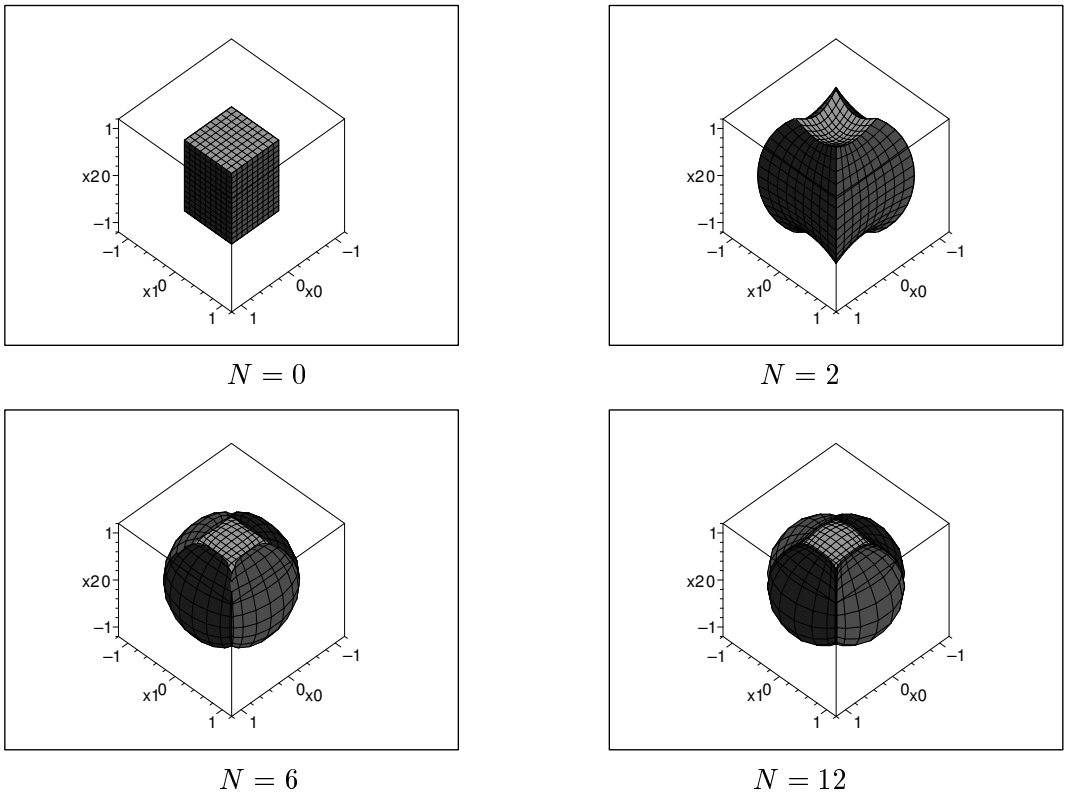

Figure 4. BKM images of the domain Ω_2

For the study of the function $g_{12}^{\{3\}}(x)$ we need to consider two sides of the original domain. For this example we consider

$$\mathcal{S}_1 := \{(x_0, x_1, x_2) \in \mathbb{R}^3 : |x_0| < 1/2, |x_1| < 1/2, x_2 = 3/4\}$$

and

$$\mathcal{S}_2 := \{(x_0, x_1, x_2) \in \mathbb{R}^3 : |x_0| < 1/2, x_1 = 1/2, |x_2| < 3/4\}.$$

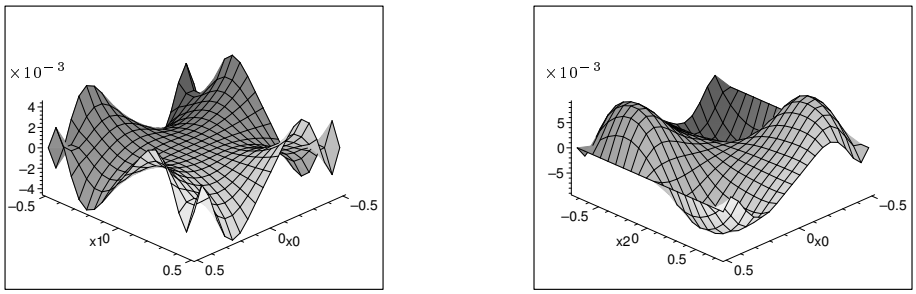

Figure 5. The function $g_{12}^{\{3\}}(x),\ x \in \mathcal{S}_1$ (on the left) and $x \in \mathcal{S}_2$ (on the right).

For the same sides of Ω_2, the graphics of the error function $\varepsilon_N(x) := 1 - ||f_N(x)||,\ x \in \mathcal{S}_1$, and $\varepsilon_N(x),\ x \in \mathcal{S}_2$ are presented on the left hand side and right hand side of Figure 6, respectively.

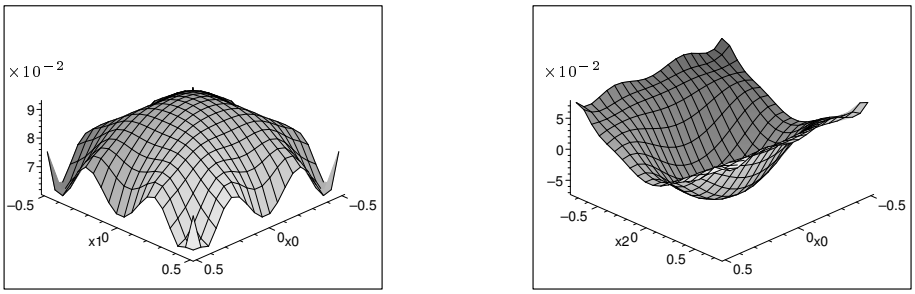

Figure 6. The function $\varepsilon_{12}(x)$.

In this case, we obtain

$$\max_{x\in\mathcal{S}_1} |g_{12}^{\{3\}}(x)| = 4.4 \times 10^{-3} \qquad \max_{x\in\mathcal{S}_2} |g_{12}^{\{3\}}(x)| = 9.0 \times 10^{-3}$$

and

$$\max_{x\in\mathcal{S}_1} |\varepsilon_{12}(x)| = 9.3 \times 10^{-2} \qquad \max_{x\in\mathcal{S}_2} |\varepsilon_{12}(x)| = 7.5 \times 10^{-2}$$

The errors $\kappa_N(0),\ N = 0,\ 2,\ 4,\ \cdots$ in the approximations $K_N(0,0)$ to the kernel function can be estimated by making use again of the results of [4]. Some of these values are listed in Table 5.

N	2	4	6	8	19	12
$\kappa_N(0)$	2.6×10^{-1}	9.6×10^{-2}	2.5×10^{-2}	7.9×10^{-3}	2.1×10^{-3}	5.7×10^{-4}

Table 5.

Finally, we draw an uniform 20×20 orthogonal grid on

$$\mathcal{S}_1(\alpha) := \{(x_0, x_1, x_2) \in \mathbb{R}^3 : |x_0| < \alpha, |x_1| < \alpha, x_2 = 3/4\}$$

and

$$\mathcal{S}_2(\alpha) := \{(x_0, x_1, x_2) \in \mathbb{R}^3 : |x_0| < \alpha, x_1 = 1/2, |x_2| < 3\alpha/4\},$$

for $\alpha = 1/3,\ 1/4,\ 1/5,\ 1/10$ and measure the associated 400 angles. The results are presented in Table 4.

	$\mathcal{S}_1$				$\mathcal{S}_2$			
$Intervals$ $(^\circ)$	$\mathcal{P}_{1/3}$	$\mathcal{P}_{1/4}$ $(\%)$	$\mathcal{P}_{1/5}$	$\mathcal{P}_{1/6}$	$\mathcal{P}_{1/3}$	$\mathcal{P}_{1/4}$ $(\%)$	$\mathcal{P}_{1/5}$	$\mathcal{P}_{1/6}$
$(25, 35)$	$--$	$--$	$--$	$--$	0.5	$--$	$--$	$--$
$(35, 45)$	$--$	$--$	$--$	$--$	2.0	$--$	$--$	$--$
$(45, 55)$	$--$	$--$	$--$	$--$	4.0	$--$	$--$	$--$
$(55, 65)$	$--$	$--$	$--$	$--$	4.0	1.5	$--$	$--$
$(65, 75)$	$--$	$--$	$--$	$--$	8.5	6.0	0.5	$--$
$(75, 85)$	14.0	5.0	$--$	$--$	13.5	16.0	15.5	$--$
$(85, 95)$	72.0	90.0	100	100	35.0	53.0	68.0	100

Table 4.

6 Conclusions

In this work we presented numerical experiments concerned with rectangular domains, but more general domains can be used. In fact, we have also similar results for ellipsoids, prisms and even a well known "difficult" L-shaped domain. Although we do not have for the moment a final theoretical justification for the remarkable results achieved by the BKM proposed, even for small values of N, we are convinced that this BKM-approach for 3 dimensional cases works and it is useful to continue the investigation in this direction. In particular, and from the computational point of view, we intend to consider: i) other choices of the basis set in step **S1** of BKM in order to get faster convergence; ii) the use of numerical quadrature rules in the Gram-Schmidt process in **S2**.

References

[1] S. Bergman. *The kernel function and conformal mapping*, volume 5 of *Math. Surveys*. Providence, R. I.: Americ. Math. Soc., 2nd edition, 1970.

[2] S. Bock. Ansätze zur Approximation einer Klasse von Abbildungen ausgewählter dreidimensionaler Strukturen der Kontinuumsmechanik auf die Kugel. Bauhaus-Universität Weimar, 2002.

[3] F. Brackx, R. Delanghe, and F. Sommen. *Clifford analysis*. Pitman, Boston-London-Melbourne, 1982.

[4] D. Constales and R. S. Krausshar. Bergman kernels for rectangular and multiperiodic functions in Clifford analysis. *Math. Methods Appl. Sci.*, 25(16-18):1509–1526, 2002.

[5] D. Constales and R. S. Krausshar. Szego and polymonogenic Bergman kernels for half-space and strip domains, and single-periodic functions in Clifford analysis. *Complex Variables Theory Appl.*, 47(4):349–360, 2002.

[6] D. Gaier. *Konstruktive Methoden der konformen Abbildung*. Springer-Verlag, Berlin, 1964.

[7] D. Gaier. *Lectures on complex approximation*. Birkhauser, Boston, 1987.

[8] K. Gürlebeck and W. Sprössig. *Quaternionic and Cliford calculus for physicists and engineers*. John Wiley & Sons, 1997.

[9] G. Jank and L. H. Tack. Conformal mapping using Bergman's method and the MAPLE system. *ACM SIGSAM Bulletin*, 25(2):18–23, 1991.

[10] D. Levin, N. Papamichael, and A. Sideridis. The Bergman kernel method for numerical conformal mapping of simply connected domains. *J. Inst. Maths Applics.*, 22:171–187, 1978.

[11] H. Malonek. Power series representation for monogenic functions in R $^{n+1}$ based on a permutational product. *Complex Variables, Theory Appl.*, (15):181–191, 1990.

[12] N. Papamichael and M. K. Warby. Stability and convergence properties of Bergman kernel methods for numerical conformal mapping. *Numer. Math.*, 48:639–669, 1986.

[13] M.V. Shapiro and N.L. Vasilevski. On the Bergman kernel function in hyperholomorphic analysis. *Acta Appl. Math.*, 46:1–27, 1997.

[14] N. L. Vasilevski. On quaternionic Bergman and Poly-Bergman spaces. *Complex Variables Theory Appl.*, 41:111–132, 2000.